

AD-A263 650

ITION PAGE

Form Approved
OMB No 0704-0188

(2)

Average 1 hour per response including the time for reviewing instructions, searching existing data sources, gathering and maintaining the data needed, and completing and reviewing the collection of information. Send comments regarding this burden estimate or any other aspect of this collection of information, including suggestions for reducing burden, to Washington Headquarters Services, Directorate for Information Operations and Reports, 1215 Jefferson Davis Highway, Suite 1205, Arlington, VA 22202-4302, DOD Form 10704-01881 Washington, DC 20503.

1. AGENCY	DATE	3 REPORT TYPE AND DATES COVERED	
4. TITLE AND SUBTITLE		5. FUNDING NUMBERS	
MODELING THE EFFECTS OF DROP DRAG AND BREAKUP ON FUEL SPRAYS		DAAL03-86-K-0174	
6. AUTHOR(S)		ALEX LIU, DAN MATHER, ROLF REITZ	
7. PERFORMING ORGANIZATION NAME(S) AND ADDRESS(ES)		DTIC ELECTE MAY 6 1993	
University of Wisconsin-Madison Engine REsearch Center 1500 Johnson Drive Madison, WI 53706		PERFORMING ORGANIZATION REPORT NUMBER	
8. SPONSORING/MONITORING AGENCY NAME(S) AND ADDRESS(ES)		10. SPONSORING/MONITORING AGENCY REPORT NUMBER	
U. S. Army Research Office P. O. Box 12211 Research Triangle Park, NC 27709-2211		ARO 24623.126-EG-01R	
11. SUPPLEMENTARY NOTES			
The view, opinions and/or findings contained in this report are those of the author(s) and should not be construed as an official Department of the Army position, policy, or decision, unless so designated by other documentation.			
12a. DISTRIBUTION/AVAILABILITY STATEMENT		12b. DISTRIBUTION CODE	
Approved for public release; distribution unlimited.			
13. ABSTRACT (Maximum 200 words)		93-09528	
<p>Spray models have been evaluated using experimentally measured drop sizes of single drops injected into a high relative velocity gas flow. The computations were made using a modified version of the KIVA-2 code. It was found that the drop drag coefficient and the drop breakup time model constant had to be adjusted in order to match the measurements. Based on these findings a new drop drag submodel is proposed in which the drop drag coefficient changes dynamically with the flow conditions. The model accounts for the effects of drop distortion and oscillation due to the relative motion between the drop and the gas. The value of the drag coefficient varies between the two limits of that of a rigid sphere (no distortion) and that of a disk (maximum distortion). The modified model was also applied to diesel sprays. The results show that the spray tip penetration is relatively insensitive to the value used for the drop drag coefficient. However, the distribution of drop sizes within sprays is influenced by drop drag. This is due to the fact that changes in drop drag produce changes →</p>			
14. SUBJECT TERMS		15 NUMBER OF PAGES	
Atomization, Drop Breakup, Drag, Sprays		16 PRICE CODE	
17 SECURITY CLASSIFICATION OF REPORT UNCLASSIFIED	18 SECURITY CLASSIFICATION OF THIS PAGE UNCLASSIFIED	19 SECURITY CLASSIFICATION OF ABSTRACT UNCLASSIFIED	20 LIMITATION OF ABSTRACT UL

in the drop-gas relative velocity. This, in turn, causes changes in the spray drop size through the drop breakup and coalescence processes. The changes occur in such a way that the net effect on the spray penetration is small over the tested ranges of conditions. These results emphasize that measurements of spray penetration are not sufficient to test and produce improved spray models. Instead, local measurements of drop size and velocity are needed to develop accurate spray models.

Modeling the Effects of Drop Drag and Breakup on Fuel Sprays

Alex B. Liu, Daniel Mather, and Rolf D. Reitz
University of Wisconsin-Madison

DTIC QUALITY INSPECTED 5

Accession For	
NTIS	CRA&I <input checked="" type="checkbox"/>
DTIC	TAB <input type="checkbox"/>
Unannounced <input type="checkbox"/>	
Justification _____	
By _____	
Distribution / _____	
Availability Codes	
Dist	Avail and/or Special
A-1	

The appearance of the ISSN code at the bottom of this page indicates SAE's consent that copies of the paper may be made for personal or internal use of specific clients. This consent is given on the condition, however, that the copier pay a \$5.00 per article copy fee through the Copyright Clearance Center, Inc. Operations Center, 27 Congress St., Salem, MA 01970 for copying beyond that permitted by Sections 107 or 108 of the U.S. Copyright Law. This consent does not extend to other kinds of copying such as copying for general distribution, for advertising or promotional purposes, for creating new collective works, or for resale.

SAE routinely stocks printed papers for a period of three years following date of publication. Direct your orders to SAE Customer Sales and Satisfaction Department.

Quantity reprint rates can be obtained from the Customer Sales and Satisfaction Department.

To request permission to reprint a technical paper or permission to use copyrighted SAE publications in other works, contact the SAE Publications Group.



All SAE papers, standards, and selected books are abstracted and indexed in the SAE Global Mobility Database.

No part of this publication may be reproduced in any form, in an electronic retrieval system or otherwise, without the prior written permission of the publisher.

ISSN 0148-7191
Copyright 1993 Society of Automotive Engineers, Inc.

Positions and opinions advanced in this paper are those of the author(s) and not necessarily those of SAE. The author is solely responsible for the content of the paper. A process is available by which discussions will be printed with the paper if it is published in SAE transactions. For permission to publish this paper in full or in part, contact the SAE Publications Group.

Persons wishing to submit papers to be considered for presentation or publication through SAE should send the manuscript or a 300 word abstract of a proposed manuscript to: Secretary, Engineering Activity Board, SAE.

Printed in USA

Modeling the Effects of Drop Drag and Breakup on Fuel Sprays

Alex B. Liu, Daniel Mather, and Rolf D. Reitz

University of Wisconsin-Madison

ABSTRACT

Spray models have been evaluated using experimentally measured trajectories and drop sizes of single drops injected into a high relative velocity gas flow. The computations were made using a modified version of the KIVA-2 code. It was found that the drop drag coefficient and the drop breakup time model constant had to be adjusted in order to match the measurements. Based on these findings, a new drop drag submodel is proposed in which the drop drag coefficient changes dynamically with the flow conditions. The model accounts for the effects of drop distortion and oscillation due to the relative motion between the drop and the gas. The value of the drag coefficient varies between the two limits of that of a rigid sphere (no distortion) and that of a disk (maximum distortion). The modified model was also applied to diesel sprays. The results show that the spray tip penetration is relatively insensitive to the value used for the drop drag coefficient. However, the distribution of drop sizes within sprays is influenced by drop drag. This is due to the fact that changes in drop drag produce changes in the drop-gas relative velocity. This, in turn, causes changes in the spray drop size through the drop breakup and coalescence processes. The changes occur in such a way that the net effect on the spray penetration is small over the tested ranges of conditions. These results emphasize that measurements of spray penetration are not sufficient to test and produce improved spray models. Instead, local measurements of drop size and velocity are needed to develop accurate spray models.

*Numbers in brackets designate References at the end of the paper.

+A.B. Liu is now with the Ford Motor Company.

SPRAYS ARE INVOLVED IN many practical applications, including spray combustion in diesel engines and port fuel injection in spark-ignited engines. In diesel engines the combustion rate is controlled by the vaporization of the drops. In spark-ignited engines, atomization quality influences the mixture preparation. In these applications the atomization process has a strong influence on fuel vaporization rates because it increases the total surface area of liquid fuel greatly.

The fundamental mechanisms of atomization have been under extensive experimental and theoretical study for many years [1]*. Information about the mechanisms of atomization is important because it is needed to optimize the performance of injection systems. Precise formulation of the drop drag and breakup processes is also essential for accurate computer modeling of sprays.

Computer models such as the time-dependent, three-dimensional computational fluid dynamics computer code, KIVA, are available to study engine sprays and combustion [2]. In some modeling studies the liquid fuel is injected as discrete parcels of drops or "blobs", whose characteristic size is equal to the orifice hole size of the injector and the injection velocity is determined from the injection rate [3,4]. The injected liquid is then broken up into atomized droplets which exchange mass, momentum and energy with the chamber gas.

Two atomization models are currently available for the breakup computations: the Taylor Analogy Breakup (TAB) model [5, 6], and the surface wave instability (wave) model [7]. The theoretical development of these models is based on linear theories, and the models contain adjustable constants that need to be determined from experimental data. The accuracy of these models is assessed by comparison with well characterized

experimental data in the present study, and the comparisons also provide information about the model constants.

The TAB model is based on Taylor's analogy [6] between an oscillating and distorting drop and a spring-mass system. The external force acting on the mass, the restoring force of the spring, and the damping force are analogous to the gas aerodynamic force, the liquid surface tension force, and the liquid viscosity force, respectively. The parameters and constants in TAB model equations have been determined from theoretical and experimental results, and the model has been applied successfully to sprays by O'Rourke and Amsden [5].

The wave breakup model considers the unstable growth of Kelvin-Helmholtz waves on a liquid surface. Reitz [7] used results from a linear stability analysis of liquid jets to describe the breakup details of the injected liquid "blobs". This stability analysis leads to a dispersion equation which relates the growth of an initial perturbation on a liquid surface of infinitesimal amplitude to its wavelength and to other physical and dynamical parameters of both the injected liquid and the ambient gas. The physical parameters in wave model are similar to those in the TAB model. This model has also been used successfully in engine spray computations [8].

In addition to the final size of atomized drops, the drop breakup time is an important parameter that must be specified by drop breakup models. In particular, the breakup time constant determines the mass change rate of a atomizing liquid drop undergoing stripping breakup. An initial perturbation level is also specified in the breakup models. This model constant has been used to account for differences between sprays from different injector geometries. For, example, a parameter called Amp0 is introduced in TAB model to account the initial oscillation amplitude of the liquid drops. An initial disturbance level also appears in the wave model as an initial wave amplitude.

In recent work by Diwakar et al. [9], measured liquid/vapor fuel distributions from an air-assisted injector were compared with computational results obtained using the TAB breakup model. Significant differences were observed between measured and calculated spatial structures within the sprays when the breakup model constants were varied. However, the selection of the model parameters such as breakup drop sizes, time constants and initial disturbance levels is difficult due to a lack of relevant experimental data.

In addition to the physics of the breakup model, another important part of spray models is the liquid drop drag coefficient. The drag effects the drop's acceleration and hence its velocity and

physical location as a function of time. In most spray modeling studies, the drop drag coefficient is specified as a function of the drop Reynolds number (based on the drop-gas relative velocity) using solid-sphere correlations [2]. Some studies have included the effect of vaporization (blowing) on the drag coefficient [8]. However, the effects of drop oscillation and distortion have not been considered previously.

In this paper, a new submodel is proposed to account for the effects of drop oscillation and distortion on the drop drag coefficient. The model uses the approach of the TAB model to estimate the distortion of drops in a high relative velocity flow. Recent experimental results of Liu and Reitz [10] are used to evaluate the drop drag model for drops undergoing breakup using both the TAB and wave breakup models. The drop breakup experiments are described first, along with other spray experiments used in the comparisons. Next, a brief review of the theories of the wave and TAB models is given. The measured drop trajectories are compared with those from the models using various model parameters. Finally, the effects of drop breakup and drop drag models on diesel spray predictions is discussed.

EXPERIMENTS FOR COMPARISON

Drop Breakup Experiments - Experiments of liquid drop breakup were carried out in an apparatus that consisted of a drop generator and an air nozzle with a converging exit, arranged in a cross flow pattern, as shown in Fig. 1 [10]. The monodisperse stream of liquid drops was generated by a Berglund-Liu drop generator [11]. The drops had an injected diameter of 170 μm and a (horizontal) velocity of 16 m/s. The liquid used was Benz UCF-I test fuel (SAE J967d specifications - density 824 kg/m³, dynamic viscosity 2.17×10^{-3} Pa.s, and surface

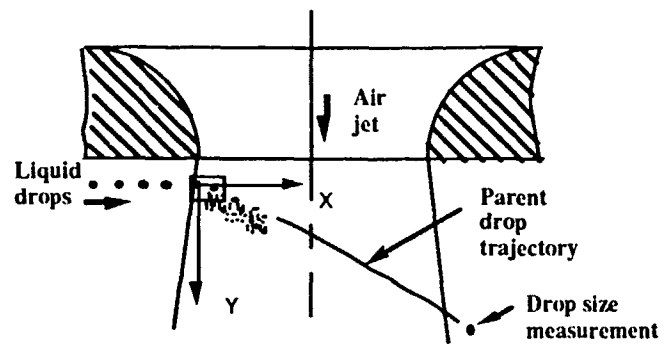


Figure 1 Schematic diagram of experiment showing coordinate system, and trajectory and drop size measurements. 170 μm diameter monodisperse liquid drop stream enters transverse air jet and breaks up. Square shows region photographed in the high magnification picture of Fig. 2.

Table 1 Experimental conditions and results

Case	Air velocity m/s	We	Re	Breakup regime
1	0	0	0	-
2	59	36	669	bag
3	72	53	816	bag
4	100	102	1133	bag
5	136	189	1541	stripping
6	152	236	1723	stripping
7	188	361	2131	surface wave
8	214	467	2425	surface wave
9	250	638	2833	surface wave

tension coefficient 0.02 kg/s^2). The air jet (vertically downward) velocity was varied between 0 and 250 m/s, and the 9 cases considered in the experiments are summarized in Table 1. The experiments were performed in atmospheric air at room temperature to avoid vaporization effects.

The contoured entrance of the air jet nozzle ($R/D=0.5$, $D=9.525 \text{ mm}$) ensured that the axial velocity profile in the jet at the point where the drops entered the jet (2 mm downstream of the air nozzle exit plane) was flat. This was confirmed by LDV velocity measurements made near the nozzle exit [12]. This ensured that mixing and shear layer effects were negligible, since the drops entering the air jet were suddenly exposed to the jet velocity in a distance of the order of the drop diameter. High magnification ($\times 56$), high speed photographs (e.g., Fig. 2) as well as conventional spray field photographs were taken of the breakup and trajectory of the drops as they entered and interacted with the transverse air jet. The breakup was recorded on 35 mm film and the drops were illuminated with a Cu vapor laser with a 10ns pulse time, adequate to freeze the breakup details.

The microscopic photographs revealed that the unstable growth of surface waves is involved in the breakup process at high relative velocities, as indicated by the arrow in Fig. 2 which shows breakup for Case 9 (air jet velocity 250 m/s). This mechanism is consistent with the mechanism of the wave breakup model [7]. Attempts have been made to compare measured wavelengths from the photographs with the wave model predictions [10], but the rapid acceleration of the drop makes the comparison difficult since the drop-gas relative velocity at the liquid surface varies with time (and space) during the breakup process. Moreover, the details of the velocity distribution within the unsteady liquid and gas boundary layers in the vicinity of the interface are not known.

However, the liquid drag coefficient can be estimated by measuring the displacement of the center of mass of the (parent) liquid drop in both

axial and radial directions on the photographs. The value found by Liu [12] for the drag coefficient at high relative velocities was $C_D=1.52$, which is close to that of a disk at high Reynolds numbers, and is also consistent with results obtained by Simpkins and Bales for drops in an incompressible flow field [13].

As seen in Fig. 2, the parent drop undergoes continuous breakup during its interaction with the air jet. The parent drop is defined as that contiguous portion of liquid with the largest mass which penetrates the furthest into the air jet (see Fig. 1). Measurements of its trajectory from the photographs provide an opportunity to check drop trajectory and breakup computations. The accuracy of the trajectory measurements relies on knowledge of the location of the edge of the air jet for a reference location. It is estimated that this was known to within 0.25 mm.

In experiments at low gas jet velocities, the parent liquid also emerged from the opposite side of the air jet, as depicted in Fig. 1. In these cases (Cases 1,2 and 3, Table 1) it was also possible to measure the parent drop's diameter using an Aerometrics phase/Doppler particle analyzer (PDPA). This data provides useful information about the outcome of the breakup process (see Fig. 1). However, at high air jet velocities the air jet momentum was such that all of the injected liquid remained within the air jet and the breakup drop sizes were too small, and their velocities were too high, to allow accurate PDPA drop size measurements for drops within the air jet. Further details of the drop breakup experiments are described in Liu and Reitz [10].



Figure 2 Photograph showing drop breakup details for Case 9, Table 1. 170 μm diameter injected drops are deflected and broken up by the 250 m/s air jet. In this photograph the drop stream moves from right to left.

Spray Experiments - Spray penetration measurements of Hiroyasu and Kadota [14] were used for the spray comparisons. In these experiments diesel fuel was injected in nitrogen gas at 300 K (i.e., a non-vaporizing spray) and the penetration of the spray tip was measured as a function of time. The ambient gas pressure was 1.0, 3.0 and 5.0 MPa for the three cases considered in the present study, Cases A, B and C, respectively. In the computations diesel fuel was simulated using tetradecane and the environment gas was initially quiescent. The initial injected drop radius was 150 μm (equal to nozzle hole radius) and the injection velocity was held constant at 102, 90.3 and 86.4 m/s for Cases A, B and C, respectively [14].

MODEL DETAILS

The computations were performed using a modified version of the KIVA-2 code, which solves the three-dimensional equations of transient chemically reactive fluid dynamics. The governing equations and the numerical solution method are discussed in detail by Amsden et al. [2].

The cylindrical computational domain for the drop breakup study is shown in Fig. 3. Drops were injected at the edge of the air jet as shown, and appropriate in-flow and out-flow boundary conditions were specified on the side, top and bottom walls. The contoured nozzle exit geometry

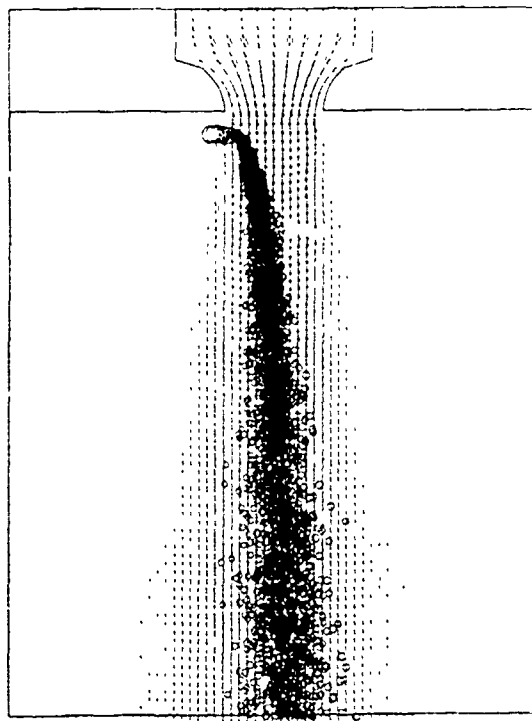


Figure 3 Computed drop locations and gas velocity vectors in the plane of the nozzle, 4 ms after the start of injection for Case 4 (air jet velocity 100 m/s). Stream of 170 μm diameter drops enters air jet from the left at 16 m/s.

was generated and the normal velocity component was specified at the air in-flow boundary. The velocity profile at the nozzle exit was found to be flat, as in the corresponding experiments. The computations were made on a three-dimensional mesh of 32x16x84 cells in the radial, azimuthal and axial directions, respectively. The cylindrical domain had a diameter of 52 mm and its length was 57 mm.

The spray computations used a two-dimensional (axisymmetric) cylindrical domain, 40 mm in diameter and 120 mm in length which was discretized using a mesh of 20x1x60 cells in the radial, azimuthal and axial directions, respectively. This mesh resolution was found to be sufficient to give adequately grid-independent results.

The spray computations were made by injecting drop parcels containing drops with sizes equal to the injected drop size (in the drop breakup study), or equal to the nozzle exit diameter (in the spray study). The breakup of the injected liquid was accounted for using the surface wave breakup and TAB models, as described below. The modifications to the liquid drop drag model necessary to account for drop distortion and oscillation are also described in this section.

Wave Breakup Model - In the wave breakup model the breakup of the parcels and the resulting drops is considered using results from a stability analysis for liquid jets. The theory considers the stability of a column of liquid issuing from a circular orifice into a stationary incompressible gas. An infinitesimal axisymmetric surface displacement is imposed on the initially steady motion, and causes small axisymmetric fluctuating pressures, and axial and radial velocity components in both the liquid and gas phases. These fluctuations are described by the continuity equation and the equation of motion, which are solved to give a dispersion equation for the wave growth rates and wavelengths [1].

The maximum growth rate, Ω , and its corresponding wavelength, Λ , are related to pertinent properties of liquid and gas [7] as

$$\frac{\Lambda}{a} = 9.02 \frac{(1 + 0.45 Z^{0.5})(1 + 0.4 T^{0.7})}{(1 + 0.87 W_{c_2}^{1.67})^{0.6}} \quad (1a)$$

$$\Omega \left[\frac{\rho_1 a^3}{\sigma} \right]^{0.5} = \frac{0.34 + 0.38 W_{c_2}^{1.5}}{(1 + Z)(1 + 1.4 T^{0.6})} \quad (1b)$$

where $Z = W_{e1}^{0.5}/R_{e1}$; $T = ZW_{e2}^{0.5}$; $W_{e1} = \rho_1 U^2 a/\sigma$; $W_{e2} = \rho_2 U^2 a/\sigma$ and $R_{e1} = Ua/v_1$.

Liquid breakup is modeled by postulating that new drops of radius, r , are formed from bulk liquid or "blobs", with characteristic radius a , with

$$r = B_0 \Lambda \quad (B_0 \Lambda \leq a) \quad (2a)$$

$$\text{or } r = \min \left\{ \frac{3\pi a^2 U / 2\Omega}{(3a^2 \Lambda / 4)^{0.33}} \right\}$$

$$\text{for } (B_0 \Lambda > a, \text{ one time only}) \quad (2b)$$

In Eq. (2a), it is assumed that (small) drops are formed with a drop size proportional to the wavelength of the fastest growing or most probable unstable surface wave. The value of the constant $B_0=0.6$ is chosen to give agreement with data on stable drop sizes in sprays [7]. Equation (2b) applies only to low velocity liquid undergoing Rayleigh-type breakup. It assumes that the jet disturbance has frequency $\Omega/2\pi$ (a drop is formed each period) or that drop size is determined from the volume of liquid contained under one surface wave.

The characteristic size of the unstable parent bulk liquid changes continuously with time following the rate equation

$$\frac{da}{dt} = -(a - r)/\tau \quad (r \leq a) \quad (3)$$

where

$$\tau = \frac{3.726 B_1 a}{\Lambda \Omega} \quad (4)$$

and B_1 is the breakup time constant [7]. Substituting Eqs. (1a) and (1b) into Eq.(4), and considering an inviscid liquid in the low Weber number limit gives

$$\tau = 0.82 B_1 \sqrt{\frac{\rho a^3}{\sigma}} \quad (5)$$

which is the same result as derived in the TAB method for an inviscid liquid [5]. O'Rourke and Amsden [5] suggested a value of $B_1 = \sqrt{3}$.

Reitz [7] also applied the theory to the high speed drop breakup limit. In this case, for inviscid liquids at large Weber numbers, Eq. (4) becomes [7]

$$\tau = (B_1 a / U) \sqrt{\rho_1 / \rho_2} \quad (6)$$

The data of Ranger and Nicholls [15] for high speed drop breakup suggest that $B_1=8$. Reitz [7, 8] used the value of $B_1=10$ in engine spray modeling studies. Thus there is uncertainty about the value of this constant. Part of the reason for the discrepancy could be that previous analyses did not account for the acceleration of the drops after they enter the high relative velocity gas flow. This

acceleration reduces the instantaneous relative velocity between the drop and the gas, leading longer wavelengths and longer breakup times. This phenomenon is considered in the present study since the acceleration of the drops is computed in the model.

TAB Breakup Model - The TAB breakup model considers a liquid drop to be analogous to a spring-mass system (Taylor's analogy), and the drop breakup is due to an increase in the amplitude of the drop oscillation. The oscillation of the drop surface is described by a second order ordinary differential equation

$$\ddot{y} = \frac{C_F \rho_2 W^2}{C_b \rho_1 a^2} - \frac{C_k \sigma}{\rho_1 a^3} y - \frac{C_d \mu_1}{\rho_1 a^2} \dot{y} \quad (7)$$

which is similar to that of a damped, forced harmonic oscillator. In Eq. (7), $y = x/C_b a$, where x is the displacement of the equator of the drop from its equilibrium position. In the implementation of O'Rourke and Amsden [5], breakup occurs if and only if $y > 1$. As can be seen from Eq. (7), y is a function of the flow conditions and both the liquid and gas properties.

Equation (7) can be solved analytically for constant relative velocity, W , between the drop and the gas,. The constants, C_F , C_k , C_d , and C_b , were obtained by O'Rourke and Amsden [5] by comparing experimental and theoretical results, and their values are: $C_k=8$, $C_F=1/3$, $C_d=5$, and $C_b=1/2$. More details are given in O'Rourke and Amsden [5].

The above values of the constants imply that the breakup time proportionality constant, B_1 , is equal to $\sqrt{3} = 1.73$ for high Weber numbers and inviscid liquids, which is significantly different from the value previously used in the wave model [7]. Although the computational results are sensitive to the value of the breakup time proportionality constant in both wave and TAB models, it should be noted that the actual breakup rate may be different with the same breakup time constant value because the physics and implementation details of the two models are different. Further comparisons with experiments are needed to determined the model constants more precisely. This is considered in the present study.

Drop Drag Model - The equation of motion of a spherical drop moving at relative velocity W in the gas is

$$\rho_1 V \frac{d^2 \bar{X}}{dt^2} = C_d A_f \rho_2 W^2 / 2 \quad (8)$$

where X , V and A_f are the drop's vector position, volume and frontal areas, respectively. The drop drag coefficient is usually given by that of a rigid sphere [2]

$$\frac{24}{Re} \left(1 + \frac{1}{6} Re^{2/3}\right) \quad Re \leq 1000$$

$$C_d = \begin{cases} 0.424 & Re > 1000 \end{cases} \quad (9)$$

However, when a liquid drop enters a gas stream with a sufficiently large Weber number, it deforms and is no longer spherical as it interacts with the gas, (see, for example, Fig. 2). This has also been observed experimentally by many researchers, e.g., [10], [15] and [16]. Taylor [6] predicted the shape of a deformed liquid drop. He proposed that the liquid drop distorts into a plano-convex lenticular body of the same volume as that of the original spherical drop due to the acceleration of the gas stream. The diameter of the flattened drop is about 3.76 times that of the original sphere. The shortcoming of this simple approach is that other important parameters, such as the liquid surface tension, viscosity, and the flow conditions, are not included, and the deformed drop has a constant shape even though the flow conditions may be changing.

At high relative velocities, the liquid drop deforms as it breaks up, and its drag coefficient should be a function of its Reynolds number and its oscillation amplitude. Based on these observations, the Taylor analogy model equation was used in the present study to predict the amplitude of the surface deformation as the drop interacts with the gas, as depicted in Fig. 4. The liquid drop drag coefficient was then related empirically to the magnitude of the drop deformation. This approach was considered to be adequate in order to assess the influence of a dynamically varying drag coefficient on spray behavior.

In the computations the amplitude of the drop's surface oscillation was calculated using Eq. (7). Since the drag coefficient of a distorting drop should lie between the lower limit of a rigid sphere, Eq. (9), and the upper limit of a disk, 1.52, a simple expression was adopted for the drag coefficient:

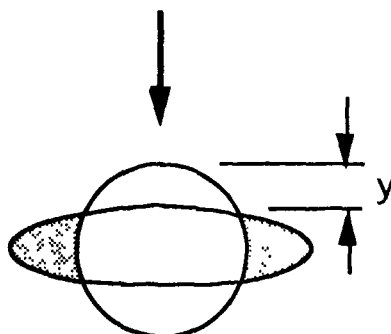


Fig. 4 The dynamic drag model accounts for the distortion of drops due to the flow by using Taylor's analogy between a drop and a spring-mass system.

$$C_d = C_{d,sphere} (1 + 2.632y) \quad (10)$$

where y is the drop distortion computed from the TAB model, Eq. (7). In the limits of no distortion ($y=0$) and maximum distortion ($y=1$), the rigid sphere and disk drag coefficients are recovered, respectively.

In contrast to the method of the TAB breakup model, the drop was not (instantaneously) broken up once the maximum distortion limit ($y=1$) was reached. Instead, breakup was considered throughout the drop lifetime using the wave model, i.e., the surface wave breakup model was always applied, regardless of the magnitude of the drop distortion. The solution of Eq. (7) was also obtained throughout the drop lifetime in order to monitor when the distortion parameter dropped below $y=1$. This made it possible to account for the tendency of a fully deformed drop to revert back to its undeformed spherical state as it accelerates up to the gas velocity and the relative velocity between the drop and the gas decreases.

The linear variation of the drag coefficient with drop deformation specified in Eq. (10) is an uncertainty in the present model which needs to be verified experimentally. However, the fact that the drop breaks up continuously while it deforms would make these experiments difficult. There have been studies of drop deformation in the absence of breakup. Ruman [17] predicted the distortion and drag coefficient of liquid drops as a function of the flow conditions. In their approach, the shape of the liquid drop was determined iteratively from computed surface pressure distributions using curve fits of measured pressure distributions around bodies of various shapes. However, several considerations limit the application of their model to the present study. First, their calculations assume freely falling drops at their terminal velocity (i.e., gravitational acceleration only), while drop acceleration is an important factor in sprays. Second, the range of Weber numbers considered by Ruman et al. was too small for spray computations ($We < 20$). Also, the approach is computationally very intensive since the pressure distribution around each drop in the spray must be resolved.

RESULTS AND DISCUSSION

A comparison of the experimental and computed parent drop trajectories was made using both the TAB and wave atomization models, together with the standard and the dynamically varying drop drag models. In addition, the models were applied to computations of diesel sprays. These results are discussed next.

Drop Breakup

Figure 3 shows computed drop locations and gas velocity vectors in the plane of the nozzle, 4 ms after the start of injection for Case 4 which has a gas velocity of 100 m/s at the air nozzle exit. The 170 μm diameter drop stream enters the air jet at 16 m/s from the left, 2 mm below the air nozzle exit face. The drops soon begin to breakup and are deflected by the air flow. For the computations of Fig. 3 drop breakup was modeled using the wave breakup model, and the dynamically varying drop drag coefficient model was employed.

Details of the deformation of a drop as a function of the horizontal distance, X , that it penetrates into the air jet are given in Fig. 5. The liquid drop Reynolds number and the distortion parameter, y , are shown in Fig. 5a. The drop size and the instantaneous drag coefficient are plotted in Fig. 5b. These results apply to an individual drop interacting with the flow.

The (parent) drop diameter is seen in Fig. 5b to decrease continuously as the drop penetrates into the air jet due to (stripping) breakup of the liquid, and breakup ceases beyond about $X=2$ mm. The Reynolds number increases rapidly to a peak value due to the increase in the relative velocity between the drop and the gas as the drop enters the air jet. The Reynolds number then decreases, following the trend of the drop size variation, with fluctuations due to the gas turbulence.

The drop distortion parameter soon increases to the fully deformed drop maximum value of $y=1$, and remains at this value until the drop size is reduced sufficiently by the breakup process, and

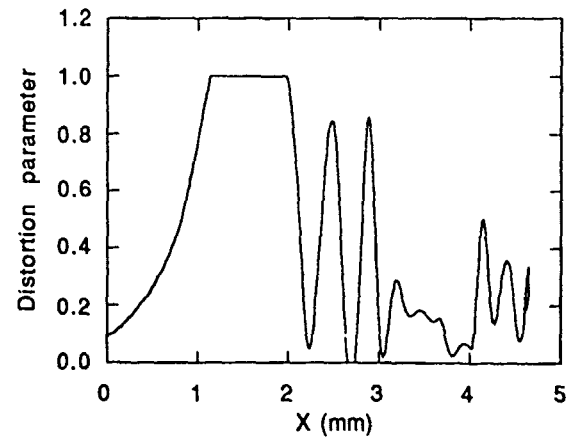
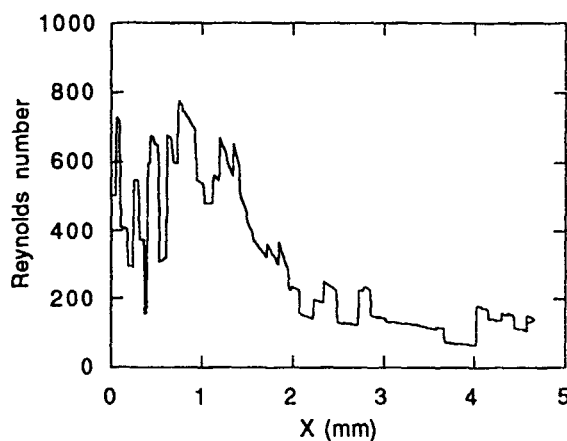


Figure 5a Drop Reynolds number and distortion parameter as a function of horizontal penetration distance, X , into the air jet. Case 4, dynamic drag and wave breakup model with $B_1=1.73$.

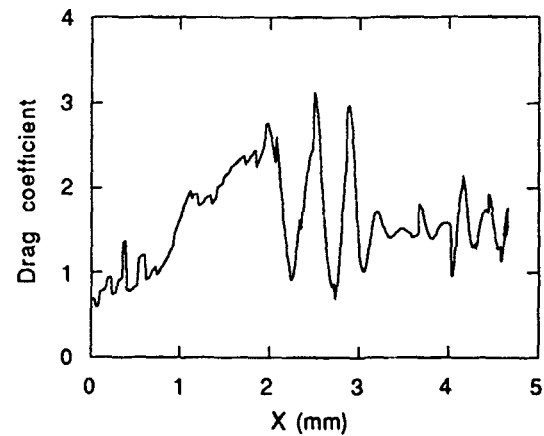
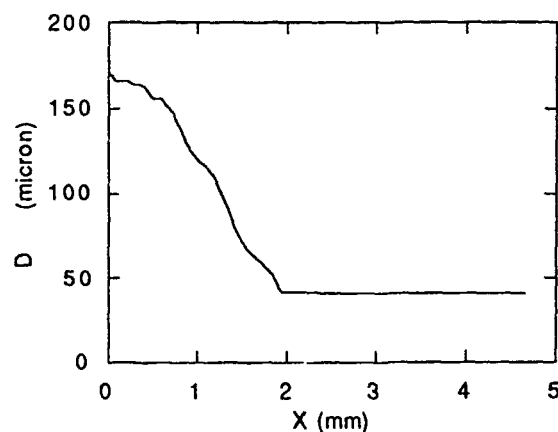


Figure 5b Drop diameter and drag coefficient as a function of horizontal penetration distance, X , into the air jet. Case 4, dynamic drag and wave breakup model with $B_1=1.73$.

(or) the drop-gas relative velocity is reduced by the acceleration of the drop. The distortion parameter then decreases. The decrease is accompanied by large fluctuations indicating that the final parent drop is only marginally stable. Even after drop breakup ceases, oscillations are still visible in the drop drag coefficient due to the drop surface oscillations. These fluctuations are caused by the interaction of the liquid drops with the turbulent eddies of the air jet.

The trajectory measurements of the experiments, Cases 2, 4, and 9, which cover the various breakup regimes observed in the experiments as indicated in Table 1 [10], were chosen for comparison with the computations. As mentioned earlier, drop size measurements were only possible at low air velocities when the liquid drops were able to penetrate out of the opposite side of the air jet (see Fig. 1). In these cases (Cases 2 and 3) the measured drop size of those drops with the longest penetration (the parent drops) were also compared with the computations.

The trajectory of a single atomizing liquid drop is effected by both its breakup rate and the drag forces acting on it. In the present computational models, these two effects are represented by the breakup time model constant, B_1 , and the drop drag coefficient, C_d , respectively. In order to validate spray models and their parameters, both the trajectory and size data should be compared with experimental data simultaneously. This is not possible in practical sprays because of a lack of accurate size and position measurements.

The experimentally measured trajectories are compared with the corresponding computations in Figs. 6 and 7 for the TAB and wave breakup models, respectively. The results in Figs. 6 to 8 represent long time averages of the corresponding computed quantities. In this case the trajectories of many drops were averaged for a time interval of about 3 ms, starting after the first drops exited the computational domain, i.e., when steady state was reached. This procedure was adopted in order to account for the influence of the gas turbulence on the drops.

The TAB model computations were made using the standard sphere drop drag coefficient, Eq. (9). As can be seen in Fig. 6a (Case 2, air velocity 59 m/s), there is excellent agreement between the drop trajectory predicted by the TAB model and the measurement with the initial oscillation parameter set equal to zero, i.e., $Amp0=0$. The initial oscillation amplitude was also varied to assess the sensitivity of the predictions to this model constant. The results in Figs. 6b and 6c show trajectory calculations made with $Amp0=0$ and 2, for Cases 4 and 9 (air velocity 100 m/s and 250 m/s, respectively). The larger $Amp0$ value leads to faster drop breakup, and the results confirm that

$Amp0=0$ is the best selection. As $Amp0$ is increased beyond $Amp0=2$, the computed drop trajectory deviates significantly from the measured data.

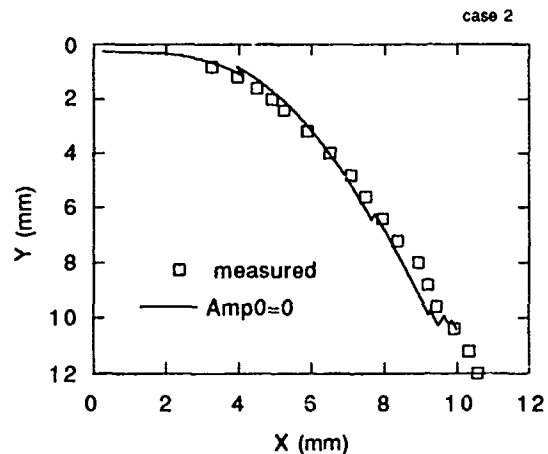


Figure 6a Comparison of TAB model and measured drop trajectory for Case 2. Initial oscillation amplitude $Amp0=0$.

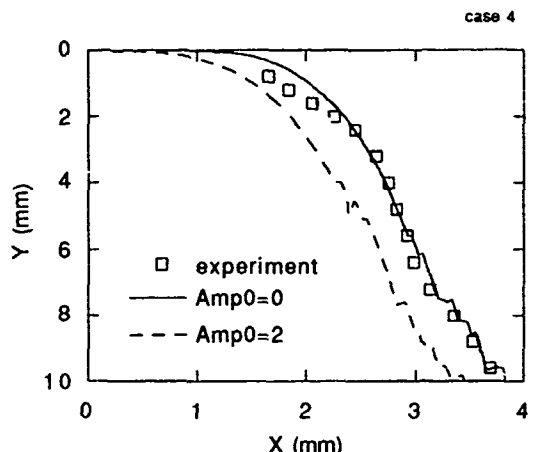


Figure 6b Comparison of TAB model and measured drop trajectory for Case 4. Solid line - $Amp0=0$, dashed line - $Amp0=2$.

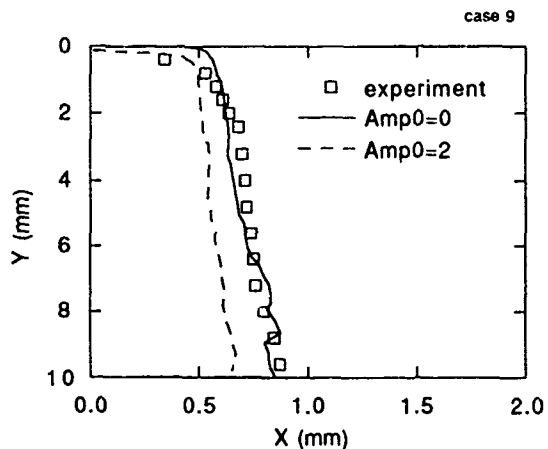


Figure 6c Comparison of TAB model and measured drop trajectory for Case 9. Solid line - $Amp0=0$, dashed line - $Amp0=2$.

The TAB model results were found to be relatively insensitive to the value of the drop drag coefficient. This is because at high gas velocities the drop distortion parameter, y , soon reaches its maximum value (equal to one, see for example Fig. 5a), and the parent drop is then instantaneously broken up into small drops. These small drops have small inertia and quickly accelerate up to the gas velocity. There is no identifiable large parent drop that survives and continues to interact with the gas, as is the case with the wave breakup model.

Another result of the absence of the surviving parent drop is that the final drop size predicted by the TAB model is smaller than that predicted by the wave model. This is shown in Fig. 8 which presents the computed variation in drop Sauter mean diameter as a function of residence time in the air jet for Cases 2 and 3 (cf. Fig. 4). Also shown is the measured drop diameter after the drops leave the opposite side of the air jet (PDPA - solid symbols at the right of the plot). The TAB model is seen to underestimate the measured final drop sizes. In fact, the results in Figs. 6 and 8 indicate that breakup effects are overestimated, and the effect of the drag coefficient is underestimated by the TAB model. The combination of these two effects could give either good agreement in the parent drop trajectory, or in its final drop size, but not both at the same time.

Computational results obtained using the wave model together with the standard drop drag and the dynamically varying drop drag models are presented in Figs. 7a, b and c for Cases 2, 4, and 9, respectively. As shown in Fig. 7a, the dynamically varying drop drag coefficient produces better results than the standard rigid sphere drag coefficient model. However, the trajectory results are also influenced by the rate of mass loss due to breakup. The computations of Fig. 7a were made using the breakup time constant, $B_1=1.73$. The use of $B_1=10$, which has been previously recommended for spray computations [7, 8], gave poorer agreement with the experiments as shown also in Figs. 7b and 7c (Cases 4 and 9, respectively) for computations made with the standard drag coefficient. Use of the value $B_1=1.73$ increases the drop breakup rate and the parent drops are thus accelerated up to the gas velocity more readily since they lose their mass more rapidly.

Other computations showed that it was not possible to match the measured drop trajectory and the final drop size simultaneously by varying the drop breakup time constant alone, without also increasing the value of the drop drag coefficient beyond the rigid sphere value [10]. However, the results in Figs. 7a, 7b and 7c show that the use of the dynamically varying drag coefficient (with $B_1=1.73$) gives adequate agreement with the measured trajectories in all cases (i.e., within the

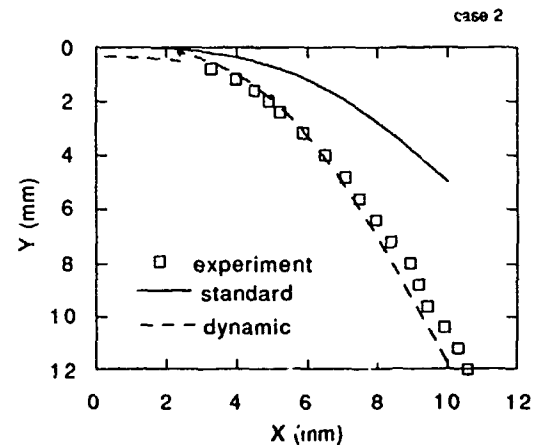


Figure 7a Comparison of wave breakup model and measured drop trajectory for Case 2. Solid line - standard drop drag, dashed line - dynamic drag. Breakup model constant $B_1=1.73$.

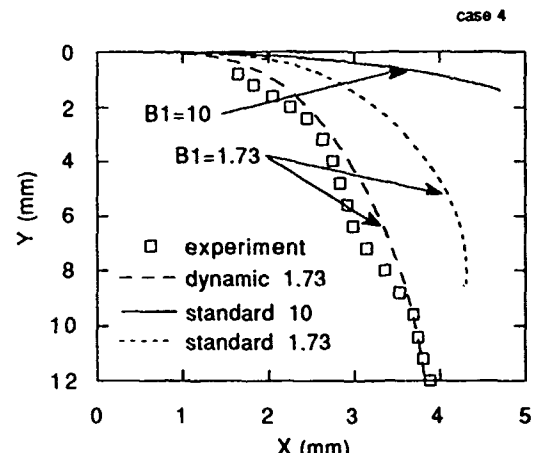


Figure 7b Comparison of wave breakup model and measured drop trajectory for Case 4. Dashed line - dynamic drag, $B_1=1.73$. Solid and dotted lines - standard drop drag with $B_1=10$ and 1.73, respectively.

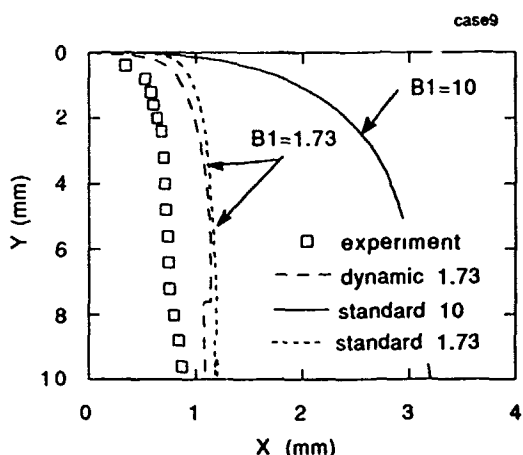


Figure 7c Comparison of wave breakup model and measured drop trajectory for Case 9. Dashed line - dynamic drag, $B_1=1.73$. Solid and dotted lines - standard drag with $B_1=10$ and 1.73, respectively.

Application to Diesel Sprays

A study was made to assess the influence of drop breakup and drag models on diesel spray predictions. The standard and dynamically varying drag models were applied to the three sprays of Hiroyasu and Kadota [14] Cases A, B and C, described earlier. The computations were made using the wave breakup model with breakup constant, $B_1=1.73$.

The results in Fig. 9 show spray-tip penetration versus time predictions together with the measurements. As can be seen, the spray penetration is insensitive to the drop drag model in all cases. In addition, there is excellent agreement between the predictions and the measurements.

The fact that similar agreement was also found by Reitz [7] for the same sprays with the same wave breakup model but with $B_1=10$, and by O'Rourke and Amsden [5] with the TAB model, indicates that spray-tip penetration is also insensitive to the breakup model details. These findings are consistent with other results of Reitz and Diwakar [4], who found that spray penetration is controlled mainly by the rate of momentum transfer between the drops and the gas, and this is controlled by the turbulence model.

Although the drop drag coefficient has relatively little effect on spray penetration, it does influence the distribution of drop sizes within the spray. This can be seen in Figs. 10a, b and c which show the variation of Sauter mean drop diameter (averaged over each spray cross-section) with distance from the nozzle exit for Cases A, B and C, respectively, using the standard and dynamic drag

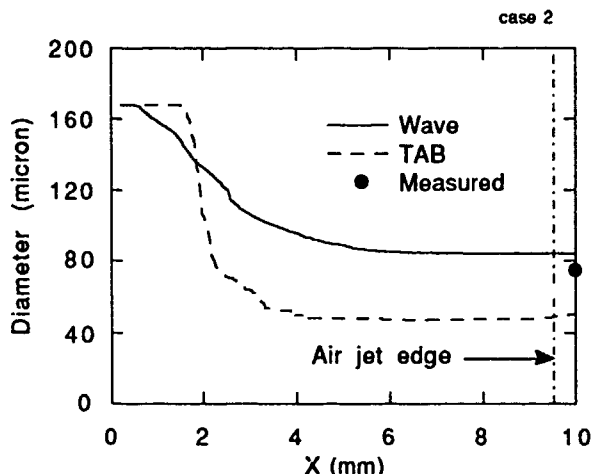


Figure 8a Predicted drop Sauter mean diameter variation with distance across the jet for Case 2 using the wave (solid line) and TAB (dashed line) models. Solid circle shows PDPA measured drop diameter outside air jet.

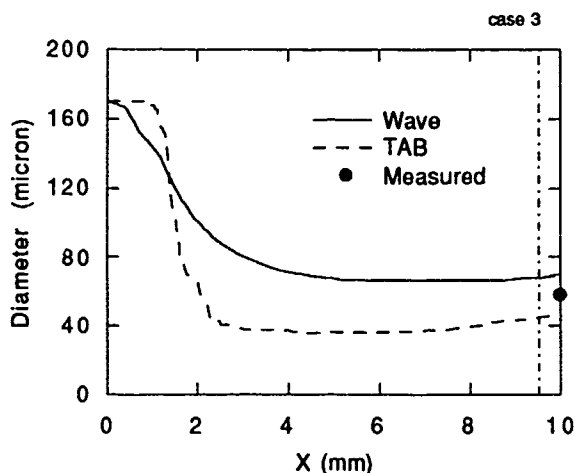


Figure 8b Predicted drop Sauter mean diameter variation with distance across the jet for Case 3 using the wave (solid line) and TAB (dashed line) models. Solid circle shows PDPA measured drop diameter outside air jet.

uncertainty in the measured trajectory data). The effect of the drag model is most pronounced at low gas velocities. As seen in Fig. 7c, at very high gas velocities for results with the same breakup model constant, drop breakup occurs so quickly that the effect of the drag coefficient on the drop trajectory is minimal.

In addition, as seen in Figs. 8a and 8b, the computed drop sizes calculated using the combination of the wave breakup model (with $B_1=1.73$) together with the dynamic drag model, are also in excellent agreement with the PDPA measurements. This drop size comparison serves as an independent check on the performance of the combination of breakup and drag models.

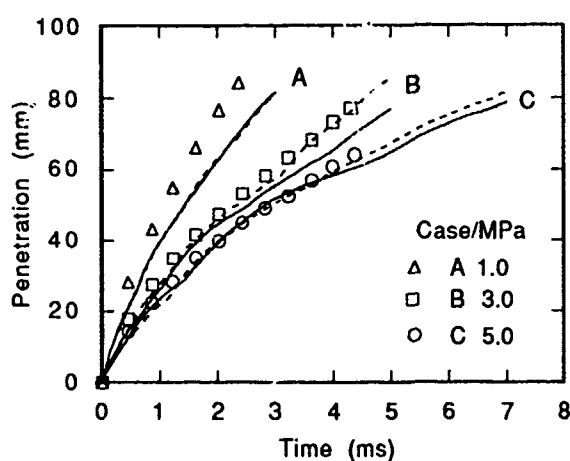


Figure 9 Comparison of predicted (lines) and measured (symbols) spray tip penetration for Cases A, B and C (1, 3 and 5 MPa gas pressure, respectively). Wave drop breakup model with $B_1=1.73$. Solid line - standard drag, dashed line - dynamic drag model.

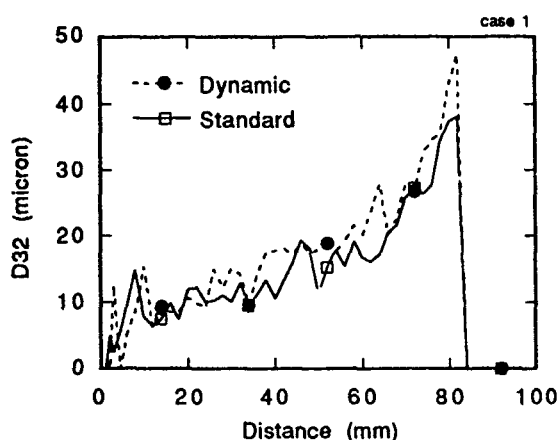


Figure 10a Effect of drop drag model on average spray drop size versus distance from the nozzle for Case A (1 MPa gas pressure). Wave drop breakup model with $B_1=1.73$. Solid line - standard drag, dashed line - dynamic drag model.

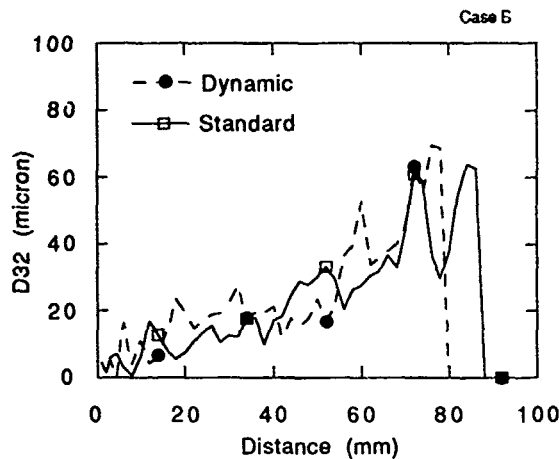


Figure 10b Effect of drop drag model on average spray drop size versus distance from the nozzle for Case B (3 MPa gas pressure). Model as in Fig. 10a.

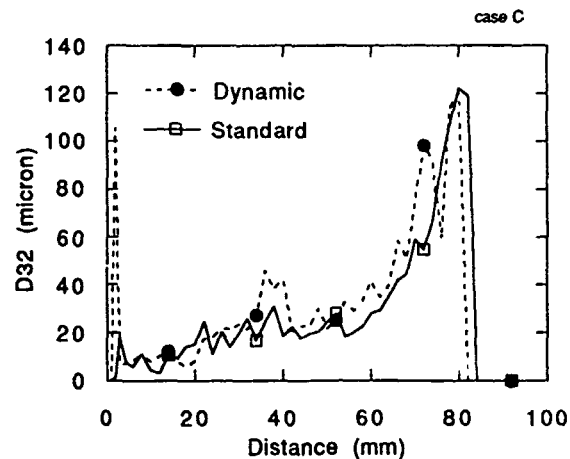


Figure 10c Effect of drop drag model on average spray drop size versus distance from the nozzle for Case C (5 MPa gas pressure). Model as in Fig. 10a.

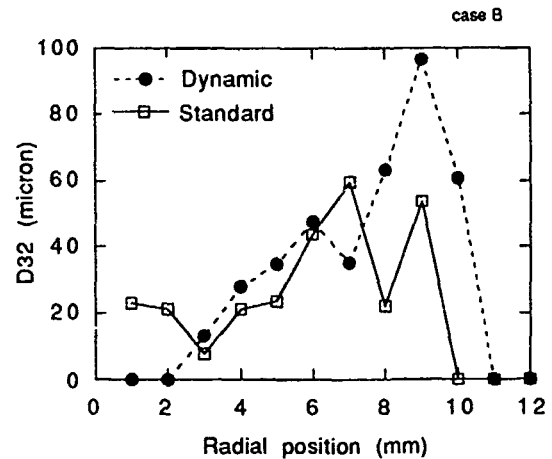


Figure 11 Effect of drop drag model on radial drop Sauter mean diameter distribution 60 mm downstream of the nozzle for Case 3 (5 MPa gas pressure). Model as in Fig. 10a.

models. The results are shown at 6 ms after the beginning of the injection. The increase in drop size with distance is due to the effect of drop collision and coalescence [4]. In general, the dynamic drag model (dotted lines) predicts larger drops than the standard drag model. The results in Fig. 11 show the predicted influence of the drop drag model on the radial Sauter mean drop size distribution, 60 mm downstream of the nozzle for Case C. The dynamic drag model is seen to predict larger drops at the edge of the spray than the standard drag model.

A series of simplified model computations were made in order to help explain why the rate of momentum transfer from the liquid to the gas in sprays with different drop size distributions is such that different models can give sprays with the same tip penetrations. Three different computations were made for Case B using exaggerated values of the drop drag coefficient where the standard rigid sphere drag coefficient was simply multiplied by a constant value equal to 0.25 and 4.0 times the standard value. Consistent with the results of Fig. 9, the results in Fig. 12a show that the spray-tip penetration is insensitive to the value used for the drop drag coefficient, in spite of the factor of 16 range of drag coefficient used in the three computations. This somewhat surprising result is apparently due to the fact that changes in the drag coefficient produce changes in the drop-gas relative velocity which, in turn, cause changes in the spray drop size.

The changes in the spray drop size due to the influence of the drag coefficient are shown in Fig. 12b, which presents the average Sauter mean diameter as a function of distance from the nozzle exit for the above three cases. The results show, with a high drag coefficient for example, that the breakup and coalescence models lead to larger drops

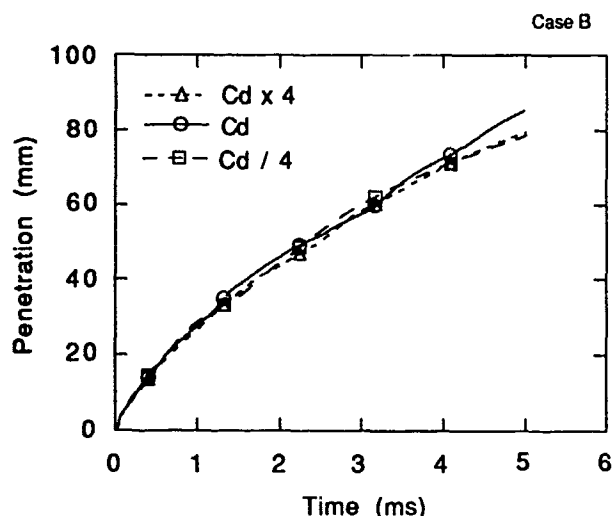


Fig. 12a Computed spray tip penetration versus time with reduced ($\times 0.25$) and increased ($\times 4$) standard drag coefficient.

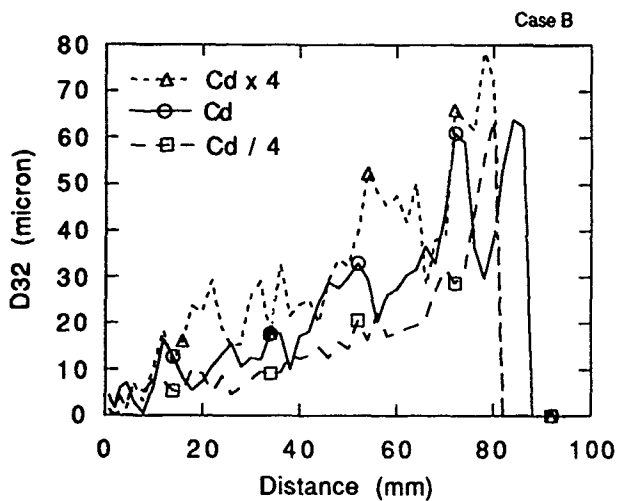


Figure 12b Computed Sauter mean diameter variation with distance from the nozzle with reduced ($\times 0.25$) and increased ($\times 4$) standard drag coefficient.

since increased drag lowers the relative velocity between the gas and the drops. These larger drops have correspondingly higher momentum, with the result that the spray-tip penetration is independent of the drop drag coefficient.

SUMMARY AND CONCLUSIONS

Drop breakup and trajectory measurements, and spray penetration data, have been compared with computations made using a modified version of the multi-dimensional KIVA-2 code. Spray atomization was modeled using a wave breakup model that is based on results from jet stability analysis, and also using KIVA's TAB model (Taylor Analogy Breakup).

The wave model was found to give good results for both drop trajectories and breakup drop sizes. The best results were obtained with a smaller value of the breakup time model constant ($B_1=1.73$) than previously used in spray computations (i.e., $B_1=10$).

The drop trajectory and size measurements, together with high magnification photographs, indicate that drop distortion should be accounted for in sprays. Accordingly, a modified drop drag model is proposed in which the drop drag coefficient changes dynamically with the flow conditions during the drop lifetime. In the model the value of the drag coefficient varies between the limits of a rigid sphere (no distortion) and a disk (maximum distortion). The drop distortion is computed using the Taylor analogy between a drop and a spring-mass system, and the breakup process is described using the wave model.

The TAB breakup model was also found to give good predictions of drop trajectories (with the model constant $Amp_0=0$), but the model underpredicted measured the breakup drop sizes considerably. The TAB results were thus relatively insensitive to the drop drag model since small drops have low inertia, and they quickly accelerate up to the gas velocity.

The wave breakup and dynamic drag models were also applied to diesel sprays. The results confirm previous studies that show that spray-tip penetration is relatively insensitive to drop breakup and drag models. However, the distribution of drop sizes within the sprays was found to be influenced by the model details. This is due to the fact that drop drag changes the drop-gas relative velocity, and this changes the spray drop size, since the drop breakup and coalescence processes depend on the velocity. However, these changes occur in such a way that the net effect on the spray penetration is small. These results emphasize the need for measurements of drop size and velocity for the development of accurate computer models of sprays.

ACKNOWLEDGEMENTS

Support for this work was provided by S.C. Johnson & Son, Inc., NASA-Lewis grant NAG 3-1087 and Army Research Office contract DAAL03-86-K-0174. Funding for the computations was provided by Cray Research, Inc. and by Caterpillar, Inc.

NOMENCLATURE

a	jet radius
A _{mp0}	TAB model breakup time constant
A _f	liquid drop frontal area
B ₀	wave model drop size constant
B ₁	wave model breakup time constant
C _{b,F,k,d}	constants in Eq. (7)
C _d	drop drag coefficient
D	Nozzle exit diameter
D ₃₂	drop Sauter mean diameter
P _r	Prandtl number, $\mu_2 C_p / \lambda$
r	drop radius
R	Nozzle inlet radius
Re	Reynolds number, $2 \rho_2 U a / \mu_2$
t	time
T	Taylor parameter, $T = Z We^{0.5}$
U	relative velocity
V	liquid drop volume
W	relative velocity
We	Weber number, $\rho_2 U^2 a / \sigma$
X	radial coordinate, see Fig. 1
x	drop surface displacement
y	drop distortion parameter, Eq. (7)
Y	axial coordinate, see Fig. 1
Z	Ohnesorge number, $\mu_1 / \sqrt{\rho_1 a \sigma}$
Λ	wave length
μ	dynamic viscosity
ν	kinematic viscosity
ρ	density
σ	surface tension coefficient
τ	drop breakup time
Ω	wave growth rate

Subscripts

i 1 = liquid, 2 = gas

REFERENCES

- (1) Reitz, R.D. and Bracco, F.V. "Breakup Regimes of Round Liquid Jets," Encyclopedia of Fluid Mechanics, 1987.
- (2) Amsden, A.A., O'Rourke, P.J., and Butler, T.D., "KIVA-II. A Computer Program for Chemically Reactive Flows with Sprays," Los Alamos National Laboratory Report No. LA-11560-MS, 1989.
- (3) Reitz, R.D. and Diwakar, R., "Effects of Drop Breakup on Fuel Sprays," SAE Paper 860469, 1986.
- (4) Reitz, R.D. and Diwakar, R., "Structure of High-Pressure Fuel Sprays," SAE Paper 870598, 1987.
- (5) O'Rourke, P.J. and Amsden, A.A., "The TAB Method for Numerical Calculation of Spray Droplet Breakup," SAE Paper 872089, 1987.
- (6) Taylor, G.I., "The Shape and Acceleration of a Drop in a High Speed Air Stream," in The Scientific Papers of G.I. Taylor, ed. G.K. Batchelor, Vol.III, University Press, Cambridge, 1963.
- (7) Reitz, R.D., "Modeling Atomization Processes in High-Pressure Vaporizing Sprays," Atomisation and Sprays Tech., vol.3, P.309-337, 1987.
- (8) Gonzalez, M., Lian, Z., and Reitz, R.D., "Modeling Diesel Engine Spray Vaporization and Combustion," SAE paper 920579, 1992.
- (9) Diwakar, R., Fansler, T.D., French, D.T., Ghandhi, J.B., Dasch, C.J., and Heffelfinger, D.M., "Liquid and Vapor Fuel Distribution from an Air-Assisted Injector -An Experimental and Computational Study," SAE Paper 920422, 1992.
- (10) Liu, A.B. and Reitz, R.D., "Mechanisms of Air-Assisted Liquid Atomization," Atomization and Sprays, Vol. 3, pp. 1-21. 1992
- (11) Berglund, R.N. and Liu, B.Y.H., "Generation of Monodisperse Aerosol Standards," Env. Sci. Tech., Vol.7, P.147, 1973.
- (12) Liu, A.B., "Mechanisms of Air-Assisted Liquid Atomization," MS Thesis, University of Wisconsin-Madison, 1991.
- (13) Simpkins, P.G. and Bales, E.L., "Water-Drop Response to Sudden Accelerations," J. Fluid Mech., Vol.55, No.4, P.629, 1972.
- (14) Hiroyasu, H., and Kadota, T. "Fuel droplet size distribution in diesel combustion chamber," SAE Paper 740715, 1974.
- (15) Ranger, A.A. and Nicholls, J.A., "Aerodynamic Shattering of Liquid Drops," AIAA J., Vol.7, No.2, P. 285, 1969.
- (16) Hinze, J.O., "Fundamentals of the Hydrodynamic Mechanism of Splitting in Dispersion Processes," A.I.Ch.E. J., Vol.1, No.3, P.289, 1955.
- (17) Ruman, M.A., "A Computational model for the Prediction of Droplet Shapes and the Onset of Droplet Breakup," MS Thesis, Michigan Technological University, 1988.